Journal of Multidisciplinary Engineering Science and Technology (JMEST)
ISSN: 2458-9403
Vol. 4 Issue 2, February - 2017

Three-Dimensional modeling and simulation of planar solid oxide fuel cell

Iman Mohammad Ebrahimi
Department of Chemical Engineering
South Tehran Branch, Islamic Azad University
Tehran, Iran
ebrahimi_iman90@yahoo.com

Mohammad H. Eikani
Department of Chemical Technologies
Iranian Research Organization for Science and Technology (IROST),Tehran, Iran
Mheikani@gmail.com

***Abstract*—Since Solid Oxide Fuel Cell simulation involves a large number of parameters and complicated equations, mostly Partial Differential Equations, the situation calls for a sophisticated simulation technique and hence a Finite Element Method (FEM) multiphysics approach will be employed.**

This can provide three-dimensional localized information inside the fuel cell. For this article, COMSOL Multiphysics® version 5.2 will be used for simulation purposes because it has a Batteries & Fuel Cells module, the ability to incorporate custom Partial Differential Equations and the ability to integrate. The solid oxide fuel cell (SOFC) is one of the most promising fuel cells for direct conversion of chemical energy to electrical energy with the possibility of its use in co-generation systems because of the high temperature waste heat.

In this paper, a 3-dimensional mathematical model for one cell of planar SOFC (solid oxide fuel cells) is presented. The model is derived from the partial differential equations representing the conservation laws of ionic and electronic charges, mass, energy, and momentum. Minimizing the Ohmic drop by optimizing the cathode layer thickness is the innovation in this article. So by this optimizing we can achieve to the maximum current density. In this article improvement of solid oxide fuel cell efficiency has been investigated based on optimization parameters.

Keywords: Solid oxide fuel cells, modeling, simulation, optimization

I. INTRODUCTION

Fuel cells are electrochemical devices that convert the chemical energy stored in a fuel directly into electrical power. Solid oxide fuel cell is considered as one of the most promising energy conversion device and as an alternative of existing power generation systems. SOFCs operate at high temperatures from 600 to 1000 ℃ to ensure sufficient ion conductivity through their electrolytes which are nonconductive to electrons.[1]

Since the conversion from chemical to electrical energy is direct, less energy losses are incurred during transformation. A popular derivative of this technology is the solid oxide fuel cell.[2]

It is very important to study the effects of different parameters on the performance of Solid Oxide Fuel Cells and for this purpose the experimental or numerical simulation method can be adopted as the research method of choice [3]. Numerical simulation involves constructing a mathematical model of the Solid Oxide Fuel Cell

and use of specifically designed software programs that allows the user to retouch the model to evaluate the system performance under various configurations and in real time.[4]

SOFC system involves multiphysics phenomena, including the mass balance of diffusion and adsorption of the gases; the electronic/ionic current balance of the interconnects/ current collectors, the electrodes and the electrolyte; the heat transfer and energy balance; and the electrochemical charge transfer reactions.[5-7]

It includes the full coupling between the mass balances at the anode and cathode, the momentum balances in the gas channels, the gas flow in the porous electrodes, the balance of the ionic current carried by the oxide ion, and an electronic current balance.[7-10] A schematic diagram of a planar SOFC single cell structure is shown in Fig. [1]

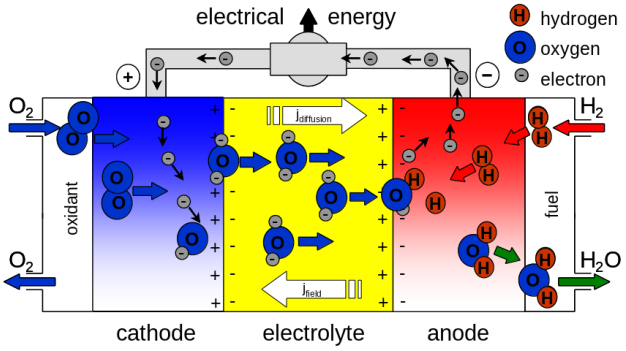

Figure 1: diagram of a planar SOFC single cell

These arise from some unknown physical properties, many reduction of the model, limitations of numerical computations, etc. Many published simulations use a simple polarization curve for validation.[11]

High SOFC performance relies on optimum electrochemical reactions and mass transport processes. These SOFC overpotentials are strongly

affected by structural parameters, such as the thickness and porosity of the electrode, and by operating parameters, such as pressure and temperature. These parameters should be taken into account to improve the design of SOFCs.[12]

II. MODELING

A. Geometry and physics

A single cell of a planar cross-flow and anode supported SOFC is considered for modeling. The model incorporates the mass, momentum and charge balance, secondary current and Butler–Volmer equations. *The model incorporates the mass, momentum and charge balance, secondary current and Butler–Volmer* equations.[13]

Fig [2] show the computational domain of the model. The domain includes a section of the ceramic membrane, both electrodes and gas flow channels in a equal configuration.

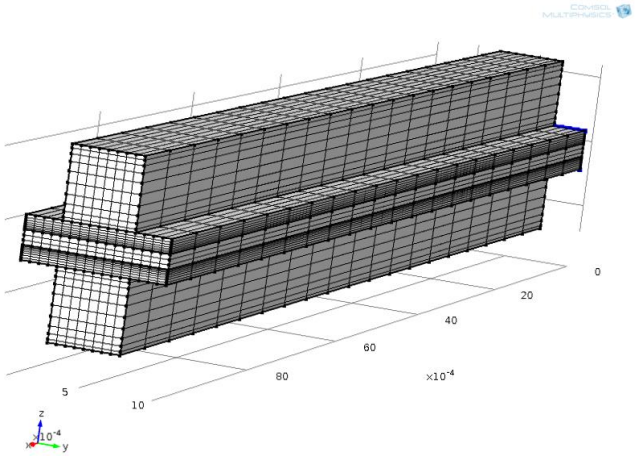

Figure 2: Computational domain of the developed SOFC model

Input parameters are shown in Table 1, which includes a temperature reference, concentration, fluid inlet velocity, inlet mole fraction and mass fraction of the components are input.

Table 1: Input parameters

parameter	Value	Scope changes
T	800℃	700-1000
cO2_ref	$2.38\ mol/\mathrm{m}^3$	-
cH2_ref	$10.78\ mol/\mathrm{m}^3$	-
U_a	$5.0363\ \mathrm{m/s}$	1-6
U_c	$13.149\ \mathrm{m/s}$	3-15
xH2	0.97	0-1
xH2O	0.03	0-0.3
xO2	0.21	0.21-1
xN2	0.79	0-0.79
wH2_in	0.78226	0-1
wH2O_in	0.21774	-
wO2_in	0.23301	-
wN2_in	0.76699	0-0.77

Governing equations bring together all the relevant parameters and variables involved the SOFC processes, and define their relationship to each other. SOFC has different types of processes happening at the same time. [14]

B. Continuity equation

$$\rho\nabla.u = 0 \tag{1}$$

In this equation, ρ is fluid density and u is velocity field.

C. Navier-Stokes equation (for incompressible fluid):

$$\rho(u.\nabla)u = \nabla.[\mu(\nabla u + (\nabla u)^T)] - \nabla P \tag{2}$$

D. Brinkman equation (for incompressible fluid):

$$\frac{\mu}{\kappa}u = \nabla.\left[\frac{1}{\varepsilon}(\mu(\nabla u + (\nabla u)^T)\right] - \nabla P \tag{3}$$

k of the fluid permeability of porous medium and ∇P represents the fluid pressure gradient. inertia term in the Brinkman equation is ignored.[15-17]

E. Maxwell-Stefan equation [18-20]

$$\left[-\rho w_i \sum \mathrm{D}_{\mathrm{ij}}^{\mathrm{eff}}\left(\nabla x_j + (x_j - w_j)\frac{\nabla P}{P}\right) + \rho w_i u\right] = S_i \tag{4}$$

The effective diffusion coefficient ($\mathrm{D}_{\mathrm{ij}}^{\mathrm{eff}}$) is calculated using the formula Knudsen as follows:[21,24]

$$\mathrm{D}_{\mathrm{ij}}^{\mathrm{eff}} = \frac{\varepsilon}{\tau}\left(\frac{1}{\mathrm{D}_{\mathrm{ij}}} \times \frac{1}{D_{iK}}\right)^{-1} \tag{5}$$

$$\mathrm{D}_{\mathrm{ij}} = 3.16 \times 10^{-8}\frac{\mathrm{T}^{1.75}}{\mathrm{P}\left(\mathrm{v_i}^{1/3} + \mathrm{v_j}^{1/3}\right)^2}\left(\frac{1}{\mathrm{M_i}} - \frac{1}{\mathrm{M_j}}\right)^{1/2} \tag{6}$$

$$D_{iK} = \frac{97}{2}d_{pore}\sqrt{\frac{T}{M_i}} \tag{7}$$

$$d_{pore} = \frac{2}{3}\frac{\varepsilon}{1-\varepsilon}d_p \tag{8}$$

And including source (S) for each component in the Maxwell-Stefan equation (Equation 4) are defined as follows: [22]

$$S_{O_2} = \frac{-J_c M_{O_2}}{4F}, S_{H_2} = \frac{-J_a M_{H_2}}{2F}, S_{H_2O} = \frac{J_a M_{H_2O}}{2F} \tag{9-10-11}$$

F. Ohm's Law equations

To express the principle of conservation of charge and ion Ohm's Law equations used are defined as follows: [23]

$$-\sigma_{el}\nabla^2\varphi_{el} = S_{el} \tag{12}$$

$$-\sigma_{io}\nabla^2\varphi_{io} = S_{io} \tag{13}$$

source term S_{el}, S_{io} represents the generation and consumption rates of species resulting from the electrochemical reaction in the SOFC.
The anode reaction layer (ARL):

$$S_{io} = -S_{el} = \mathrm{j_a} \tag{14}$$

The cathode reaction layer (CRP):

$$S_{io} = -S_{el} = \mathrm{j_c} \tag{15}$$

The electrolyte layer:

$$S_{io} = 0 \tag{16}$$

G. Butler - Vollmer equations

to express Kinetics of electrochemical reactions at the anode and cathode Butler-Vollmer equation used is as follows [13,25,26] :

$$j_a = A_{Va} j_{0,ref}^{H_2} \left(\frac{C_{H_2}}{C_{H_2,ref}}\right)^{\gamma_{H_2}} \times \left\{\exp\left(\eta_a \frac{n\alpha_a F}{RT}\right) - \exp\left(-\eta_a \frac{n(1-\alpha_a)F}{RT}\right)\right\} \quad (17)$$

$$j_c = -A_{Vc} j_{0,ref}^{O_2} \left(\frac{C_{O2}}{C_{O_2,ref}}\right)^{\gamma_{O_2}} \times \left\{\exp\left(\eta_c \frac{n\alpha_c F}{RT}\right) - \exp\left(-\eta_c \frac{n(1-\alpha_c)F}{RT}\right)\right\} \quad (18)$$

α is charge transfer coefficient and n the number of electrons involved in the electrochemical reaction is reactant per mole. For the electrochemical reaction at the anode and cathode layers (A_V) is calculated using the following equation:

$$A_V = \pi sin^2\theta r_{el}^2 n_t n_{el} n_{io} \frac{Z_{el} Z_{io}}{Z} p_{el} p_{io} \quad (19)$$

$$n_t = \frac{1-\varepsilon}{\left(\frac{4}{3}\right)\pi r_{el}^3 \left[n_{el} + (1-n_{el})\left(\frac{r_{io}}{r_{el}}\right)^3\right]} \quad (20)$$

n_{el} and n_{io} , numerical fraction of the electron conductive particles and conductive ions particles in reactive layers:

$$n_{el} = \frac{\varphi}{\left[\varphi + (1-\varphi)\left(\frac{r_{io}}{r_{el}}\right)^3\right]} \quad (21)$$

$$n_{io} = 1 - n_{el} \quad (22)$$

φ , volume fraction of particles in the electron-conducting layer is reactive.
Coordination numbers are called Z_{el} and Z_{io} around the central atom of the nearest atoms or ions in a molecule or crystal .

$$Z_{el} = 3 + \frac{Z-3}{\left[n_{el} + (1-n_{el})\left(\frac{r_{io}}{r_{el}}\right)^2\right]} \quad (23)$$

$$Z_{io} = 3 + \frac{(Z-3)\left(\frac{r_{io}}{r_{el}}\right)^2}{\left[n_{el} + (1-n_{el})\left(\frac{r_{io}}{r_{el}}\right)^2\right]} \quad (24)$$

P_{el} and P_{io} , the possibilities conductive particles electron and ion-conducting particles in the reaction layers are:

$$P_{el} = \left[1 - \left(2 - \frac{Z_{el-el}}{2}\right)^{2.5}\right]^{0.4} \quad (25)$$

$$P_{io} = \left[1 - \left(2 - \frac{Z_{io-io}}{2}\right)^{2.5}\right]^{0.4} \quad (26)$$

Z_{el-el} and Z_{io-io} are defined as follows:

$$Z_{el-el} = \frac{n_{el} Z_{el}^2}{Z} \quad (27)$$

$$Z_{io-io} = \frac{n_{io} Z_{io}^2}{Z} \quad (28)$$

η in equations 17 and 18, represents the anode and cathode activation loss, the loss due to the energy required to start a chemical reaction to occur which are defined as follows:[27-29]

$$\eta_a = \varphi_{el,a} - \varphi_{io,a} - E_{a,eq} \quad (29)$$

$$\eta_c = \varphi_{el,c} - \varphi_{io,c} - E_{c,eq} \quad (30)$$

in the above equations φ_{io} and φ_{el} respectively ion and electric potential. .$E_{a,eq}$ and $E_{c,eq}$ the equilibrium potential of the anode and cathode are reversible mode. Potential general equilibrium ($\Delta E_{eq} = E_{c,eq} - E_{a,eq}$) is obtained in the following way, which is called the Nernst equation:[30]

$$\Delta E_{eq} = E_r - \frac{RT}{nF} \ln\left[\prod_i \left(\frac{p_i}{p_0}\right)^{v_i}\right] \quad (31)$$

If reversible fuel cell to act, the Gibbs free energy will be converted into electrical energy, electrical energy necessary for the movement of electrons in the outer shell provides.[31]

$$\begin{cases} Anode : H_2 + O^{2-} \longrightarrow 2e^- + H_2O \\ athode : \frac{1}{2}O_2 + 2e^- \longrightarrow O^{2-} \end{cases} \Longrightarrow H_2 + \frac{1}{2}O_2 \longrightarrow H_2O$$

$$\Delta E_{eq} = E_r^0 + \frac{\Delta S}{nF}(T - 298.15) - \frac{RT}{nF} \ln\left(\frac{p_{H_2O}}{P_{O_2}^{1/2} . P_{H_2}}\right) \quad (32)$$

The difference between real voltage and reversible voltage is based on irreversibility. Due to the irreversibility of (voltage drops irreversible) During the process, the real work in the fuel cell is less than the maximum useful work. Actual voltage fuel cell is as follows:

$$E_{cell} = \Delta E_{eq} - \Delta E_{eq,irrev} = \Delta E_{eq} - (\Delta E_{ohmic} + \Delta E_{act}) \quad (33)$$

ΔE_{act} , general activation loss, and ΔE_{ohmic} , Ahmyk loss, which is defined by Ohm's Law:

$$\Delta E_{ohmic} = IR_{ohmic} = iA_{cell}\left(\frac{\delta_{thick}}{\sigma A_{cell}}\right) = i\frac{\delta_{thick}}{\sigma} \quad (34)$$

In this equation, i is the current density of the unit ampere per square meter.

H. Energy equations (conduction, convection and radiation)

The electrochemical oxidation consists of two half-cell reactions occurring separately in the anode and cathode, and heat is generated within the electrolyte and the electrodes. The heat generated, however, is assumed to be produced within the anode structure because the cathode and electrolyte are very thin, relative to the anode. [26,30]
The energy equation for the model is as follows. This equation is applicable to all areas, assuming that the term displacement is intended only for channels in porous media and it is ignored.

$$\nabla.(-\lambda \nabla T) = S_q - \rho C_p u.\nabla T \quad (35)$$

For thermal conductivity of porous media used are as follows:

$$\lambda = (1-\varepsilon)\lambda_{Porous} + \varepsilon\lambda_{fluid} \quad (36)$$

source term in Eq. 35, for each segment is calculated as follows.
For flow collector layer :

$$S_q = \sigma_{el}\nabla\varphi_{el}.\nabla\varphi_{el} \quad (39)$$

For the electrolyte layer :

$$S_q = \sigma_{io}\nabla\varphi_{io}.\nabla\varphi_{io} \quad (40)$$

For anode reaction layer :

$$S_q = \sigma_{el}\nabla\varphi_{el}.\nabla\varphi_{el} + \sigma_{io}\nabla\varphi_{io}.\nabla\varphi_{io} + \frac{J_a}{nF}T\Delta S + J_a\eta_a \quad (41)$$

And for the cathode reaction layer:

$$S_q = \sigma_{el}\nabla\varphi_{el}.\nabla\varphi_{el} + \sigma_{io}\nabla\varphi_{io}.\nabla\varphi_{io} + \frac{J_c}{nF}T\Delta S + J_c\eta_c \quad (42)$$

III. RESULTS AND DISCUSSION

A. *Polarization*

Polarization is a state which electrode surface potential shift from it's equilibrium value and it leads to electrochemical reaction. Polarization curve inscribes voltage changes with current density that these data are very important in evaluating the performance of fuel cell.[33]

A fuel cell with good performance should show a curve with high current density in high voltage that expresses higher output power.

As shown in figure [3] , chosen model matches with experimental results very good and it can confirm other results.

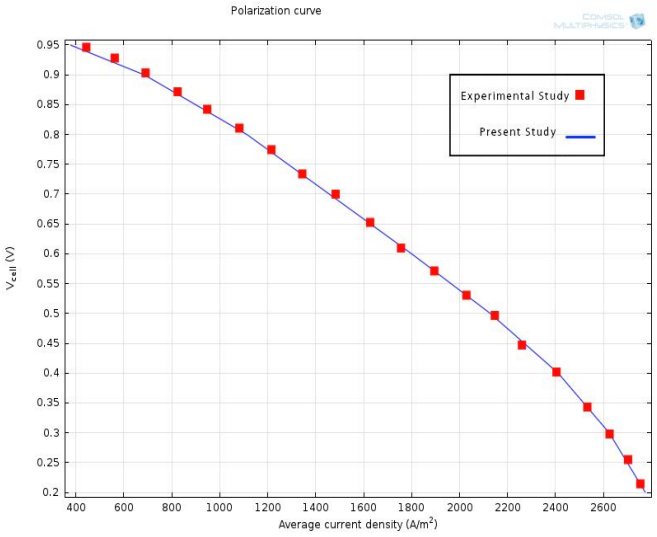

Figure 3: polarization Curve ; Comparison between the results of numerical simulation and experimental results

B. *Power curve*

Power curve shows the rate of watt that can get from this cell. Power with this formula is obtained from polarization curve and voltage multiplied by current is power. This curve in figure [5] is displayed. The produced power in this cell in certain operating condition is 11800 W/M^2.

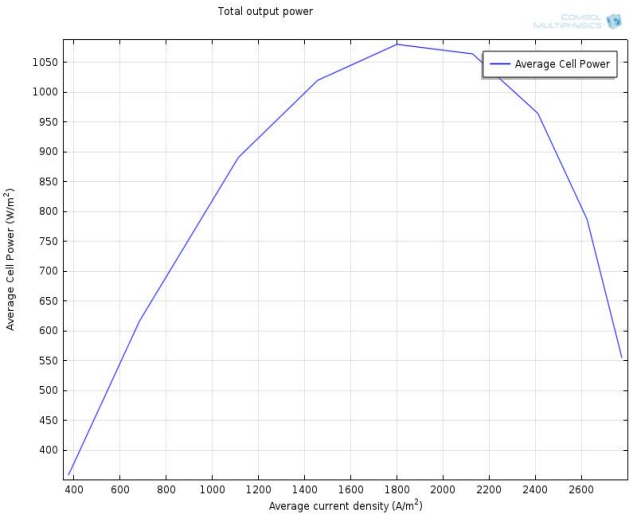

Figure 4: Fuel cell output power curve at average voltage

C. *Temperature distribution*

with consumption of it and decreasing of output concentration and produced water in electrochemical reactions lead to decrease of output temperature.
As we can see in figure [5] the chart of cell voltage according to current density has been drawn in three operating temperature. In a constant voltage as temperature increases we can see noticeable increasing in current density.

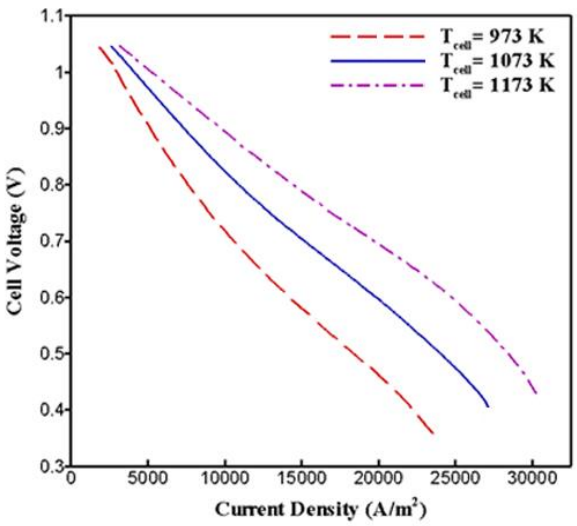

Figure 5: Cell voltage versus current density at three different temperatures

The fig [6] is about power density that is based on current density. In a constant current density as temperature increases, power density of cell increases very much, so temperature risen has positive effect on cell power.

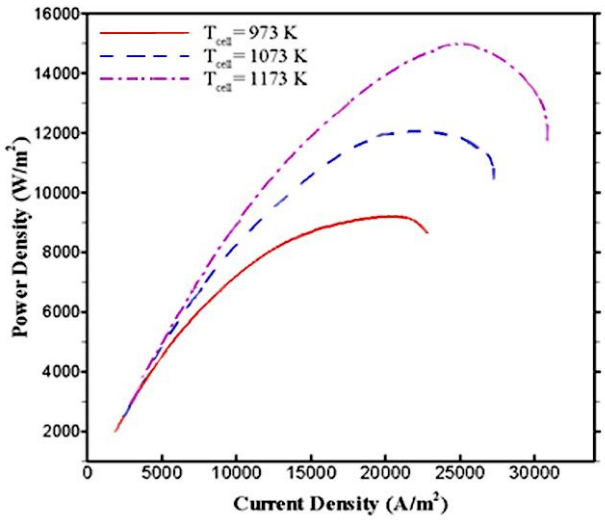

Figure 8 : Curve power density versus current density at three different temperatures

D. Concentration distribution

Figure [9] and figure [10] show hydrogen and oxygen mole fraction respectively. Figure [9] has been drawn in the voltage of 0.6 volt that shows concentration drop of hydrogen in the channel length and reaction layer (in Y direction).As a result of electrochemical reactions that occur along the channel, consumed hydrogen and produced water from oxidation of hydrogen are transferred to channel and are transferred out through fuel channel.

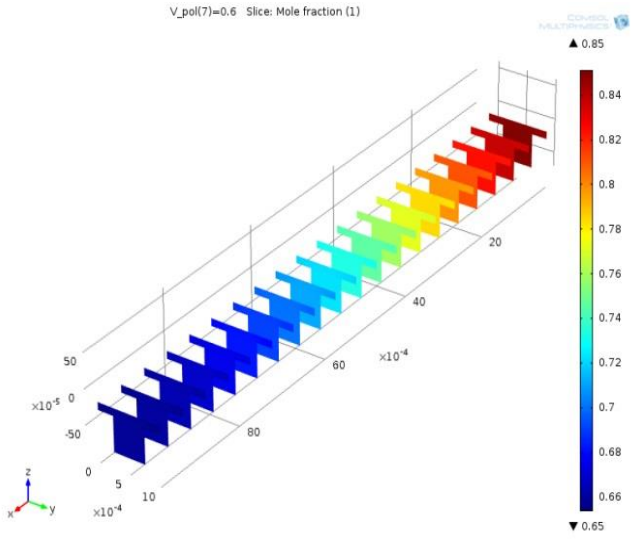

Figure 9: Hydrogen concentration distribution in the anode

In figure [10] oxygen molar concentration has been displayed in cathode in voltage of 0.6 volt. In the beginning of input, the amount of oxygen (dark red) is much and after reaction rate of oxygen 30 percent decreases and is consumed along the cell and by considering the color the rate of it in the output of channel can be seen (dark blue).

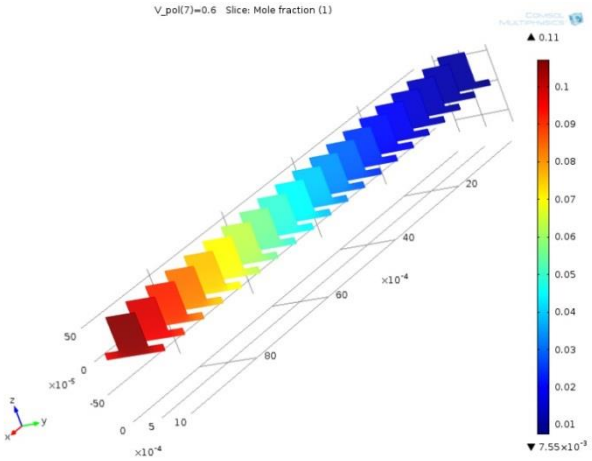

Figure 10: Oxygen concentration distribution in a cathode

three-dimensional model has been developed in order to investigate the effect of interconnect design on electrical performance and degradation process. Numerical results are discussed to evaluate the performance of different kinds of SOFC interconnect designs. The current density and temperature distributions within the fuel cell have been studied. Depending on the above results the SOFC interconnect design has been optimized for better electrical performance and higher thermal stability.

cathode electrode for all the interconnect design cases. The mass fraction of oxygen at the air entrance is high and it gradually decreases along the channel length due to the oxygen species diffusion through porous electrodes and its reduction at the electrolyte/electrode interface. It is similar to the hydrogen mass fraction in the anode channel.

The results obtained from the numerical simulations for the different interconnect designs from the previous chapter allows the optimization of interconnect design for the planar SOFC. Interconnect design have been modified to reduce the thermal gradient and improve the electrical behavior.

By optimizing the cathode thickness we can see maximum current with vertical flow .That uniform flow is moving with maximum current density .That only 5% of current has been separated from the main track. In comparison with similar papers this amount of reduction for current loss is very satisfying.

Operating temperature is one of the most important and the most effective factor in solid oxide fuel cell plate because in it has high effect on activation and ohmic drop. Each parameter that has effect on temperature of fuel cell can be effective factor in solid oxide fuel cell efficiency.

REFERENCES

[1] P. Costamagna, A. Selimovic, M. Del Borghi, G. Agnew, Chem. Eng. J. 102 (2004) 61.

[2] Momirlan M, Veziroglu T. Recent directions in world hydrogen production.

Renew Sustain Rev 1999;3:219–31.

[3] Ryan O'Hayre, Suk-Won Cha, Whitney Colella, and Fritz B. Prinz, *Fuel Cell Fundamentals*, Wiley; 2nd edition, 2009.

[4] Khaleel MA, Selman JR. In: Singhal SC, Kendall K, editors. High-temperature solid oxide fuel cells-fundamentals, design and applications. Oxford: Elsevier Science; 2003. p. 293–331.

[5] Yakabe H, Ogiwara T, Hishinuma M, Yasuda I. 3-D model calculation for planar SOFC. J Power Sources 2001;102:144e54.

[6] Autissier N, Larrain D, Van Herle J, Favrat D. CFD simulation tool for solid oxide fuel cells. J Power Sources 2004;131:313e9.

[7] Andersson M, Yuan J, Sunde´n B. SOFC modeling considering electrochemical reactions at the active three phase boundaries. Int J Heat Mass Transfer 2012;55:773e88.

[8] Andersson KMJ. Solid oxide fuel cell modeling at the cell scale. PhD thesis. Lund University; 2011.

[9] Andreassi L., Toro C., Ubertini S., 2007. Modeling carbon monoxide direct oxidation in solid oxide fuel cells. In Proceedings ASME European Fuel Cell Technology and Applications Conference, EFC2007-39057.

[10] Subhash C Singhal and Kevin Kendall, *High-temperature Solid Oxide Fuel Cells: Fundamentals, Design and Applications*, Elsevier Science; 1st edition, 2003.

[11] COMSOL Multiphysics tutorial guide. Current density distribution in Solid Oxide Fuel Cell; 2012.

[12] He Z, Birgersson E, Li H. Reduced non-isothermal model of the planar solid oxide fuel cell and stack. Energy 2014;70:478–92.

[13] Kevin Huang and John B. Goodenough, Solid oxide fuel cell technology: Principles, performance and operations, CRC Press; 1st edition, 2009.

[14] W. Kays, M. Crawford, B. Wiegand, Convective Heat and Mass Transfer, McGraw-Hill, 2005.

[15] M. M. Hussain, X. Li, I. Dincer, Journal of Power Sources,189(2009), 916-28.

[16] Y. Ji, K. Yuan, J.N. Chung, Y.C. Chen, Journal of Power Sources,161(2006), 380-91.

[17] J. H. Myung, H. J. Ko, J. J. Lee, S. H. Hyun, International Journal of Electrochemical Science, 6 (2011) , 1617-1629.

[18] B. Todd, J. B.Young, Journal of Power Sources, 110(2002), 186-200.

[19] J. H. Nam, D. H. Jeon, Electrochim Acta, 51(2006), 3446-60.

[20] E. Fuller, P. Schettler, J. Giddings, Industrial & Engineering Chemistry, 58(1966), 18-27.

[21] Ni M, Leung MKH, Leung DYC. Parametric study of solid fuel cell performance. Energy Convers Manage 2007;48(5):1525–35.

[22] B. Sunden, M. Faghri, Transport Phenomena in Fuel Cells, WITPRESS, 2005.

[23] H. Y. Zhu, R. J. Kee, Journal of the Electrochemical Society, 155(2008), B715-B29.

[24] Huangfu Y, Gao F, Abbas-Turki A, Bouquain D, Miraoui A. Transient dynamic and modeling parameter sensitivity analysis of 1D solid oxide fuel cell model. Energy Convers Manage 2013;71:172–85.

[25] Abhishek R, Tariq S , Numerical investigation of the effect of operating parameters on a planar solid oxide fuel cell, Energy Conversion and Management 90 (2015) 138–145.

[26] Lee YD, Ahn KY, Morosuk T, Tsatsaronis G. Environmental impact assessment of a solid-oxide fuel-cell-based combined-heat-and-power-generation system. Energy 2015;79(0):455e66.

[27] J.H. Koh, H.K. Seo, Y.S. Yoo and H.C. Lim, '*Consideration of Numerical Simulation Parameters and Heat Transfer Models for a Molten Carbonate Fuel Cell Stack*', Chemical Engineering Journal, Vol. 87, N°3, pp. 367 – 379, 2002.

[28] K. Sudaprasert, R.P. Travis and R.F. Martinez-Botas, '*A Computational Fluid Dynamics Model of a Solid Oxide Fuel Cell*', Proceedings of the Institution of Mechanical Engineers, Part A: Journal of Power and Energy, Vol. 219, pp. 159 - 167, 2005.

[29] Y. Wang, F. Yoshiba, T. Watanabe and S. Weng, '*Numerical Analysis of Electrochemical Characteristics and Heat / Species Transport for Planar Porous Electrode-Supported SOFC*', Journal of Power Sources, Vol. 170, N°1, pp. 101 - 110, 2007.

[30] M. Brown, S. Primdahl, and M. Mogensen. Structure/Performance Relations for Ni/Yttria-Stabilized Zirconia Anodes for Solid Oxide Fuel Cells. Journal of The Electrochemical Society, 147(2):475–485, 2000.

[31] J.-M. Klein, Y. Bultel, S.Georges, and M. Pons. Modeling of a SOFC fuelled by methane: From direct internal reforming to gradual internal reforming. Chemical Engineering Science, 62:1636 – 1649, 2007.